Acid−Base Equilibrium Constants for Ferric *trans*-1,2-Diaminocyclohexanetetraacetic Acid ($Fe^{3+}CDTA^{4-}$/$Fe^{3+}OH^{-}CDTA^{4-}$) in NaCl, Na_2SO_4, and LiCl Aqueous Solutions at 298 K

Simon Piché, Bernard Grandjean, and Faïçal Larachi*

Department of Chemical Engineering, Laval University, Ste-Foy, Canada PQ G1K 7P4

The dependence of the ferric chelate (*trans*-1,2-diaminocyclohexanetetraacetic acid) acid−base stoichiometric equilibrium constant on pH and on low-to-moderate ionic strength [$(0 < I \leq 2)$ mol kg^{-1}] was systematically studied in sodium chloride, sodium sulfate, and lithium chloride aqueous solutions at 298 K. Activity coefficient models characterizing the ionic behavior of electrolytic solutions were applied in conjunction with the measured equilibrium constant (K_C) in order to obtain the thermodynamic equilibrium constant (K) for the $Fe^{3+}CDTA^{4-}$/$Fe^{3+}OH^{-}CDTA^{4-}$ couple in slightly-to-moderately alkaline conditions ($8 \leq pH \leq 10.5$). On the basis of the Hückel, Bromley, Scatchard, and Pitzer models, the best fit over 150 K_C measurements procured an optimal log(K) value of 4.288 ± 0.022 at (298 ± 1) K. A good fit of the K_C measurements was achieved in the following ionic strength regions: Hückel ($I < 0.25$ mol kg^{-1}), Bromley ($I < 1$ mol kg^{-1}), Scatchard ($I < 1.5$ mol kg^{-1}), Pitzer ($I < 2$ mol kg^{-1}). In those instances, the predictions presented acceptable fitting capability well within the accepted limits (average absolute error on $pK_C < 0.05$).

Introduction

Chelating agents are organic molecules which have the ability to bond with multivalent cationic ions such as iron in an oxidized (Fe^{3+}) or reduced (Fe^{2+}) state. The corresponding redox reactions of simple polyaminocarboxylate complexes (i.e. $Fe^{3+}L^{n-}$/$Fe^{2+}L^{n-}$ where L^{n-} denotes an organic ligand of n- charge) have increasingly received attention over recent years. Iron chelate systems are currently used as redox catalysts for the removal of hydrogen sulfide (H_2S) contained in a broad range of sour gas streams including natural gas (eq 1).[1−4] The presence of dissolved oxygen in solutions expands the potential of this practice, as it reoxidizes the ferrous chelate product ($Fe^{2+}L^{n-}$) into reactive ferric chelate ($Fe^{3+}L^{n-}$), thus completing the redox cycle (eq 2).

$$H_2S_{(aq)} + 2Fe^{3+}L^{n-} \rightarrow S^0 + 2Fe^{2+}L^{n-} + 2H^+ \quad (1)$$

$$2Fe^{2+}L^{n-} + 0.5O_2 + H_2O \rightarrow 2Fe^{3+}L^{n-} + 2OH^- \quad (2)$$

This approach uses gas−liquid contactors in which gaseous H_2S is absorbed in neutral-to-alkaline reactive iron chelate solutions. Dissolved H_2S dissociates to form HS^- (pK_a = 7.1), which enhances the hydrogen sulfide absorption rate.[5] The use of chelating agents in such processes resides on the fact that *bare* ferric and ferrous ions inevitably precipitate in neutral-to-alkaline solutions, thus impeding the redox process from taking place. The protective ability of chelates toward sequestered iron is used therefore to prevent precipitation in these media. In most cases, the chelating agents tested in laboratories and used commercially are aminopolycarboxylic acids, such as nitrilotriacetic acid (NTA), ethylenediaminetetraacetic acid (EDTA), or *N*-hydroxyethylethylenediamine-*N*,*N*′,*N*″-triacetic acid (HEDTA). Several other chelants are also available.[3]

Philip and Brooks[4] first acknowledged that the oxidative reaction ($HS^- + 2Fe^{3+}L^{n-}$) strongly depends on the pH. Gustafson and Martell[6] and Wilkins and Yelin[7] attributed this dependence to the formation of hydroxylated ferric chelate species at high pH.

$$Fe^{3+}L^{n-} + 2OH^- \leftrightarrow Fe^{3+}OH^-L^{n-} + OH^- \leftrightarrow Fe^{3+}(OH^-)_2L^{n-} \quad (3)$$

Each species is thought to have contrasting reactivity with the hydrosulfide ion (HS^-). For example, Demminck and Beenackers[2] have demonstrated that $Fe^{3+}OH^-EDTA^{4-}$ reacts significantly with HS^-, corresponding in fact to several orders-of-magnitude over the reactivity of its non-hydroxylated counterpart ($Fe^{3+}EDTA^{4-}$). For that reason, careful knowledge of the species concentration distribution becomes crucial for accurate elaboration of reaction mechanisms. Such a distribution of ferric chelate species is controlled by acid−base thermodynamic equilibrium, which is known to be largely influenced by temperature, pH, ionic strength, and the type of electrolytes.

In this work, the acid−base thermodynamic equilibrium constant (K) for a typical ferric chelate, *trans*-1,2-diaminocyclohexanetetraacetic acid (CDTA), represented by the non-hydroxylated ($Fe^{3+}CDTA^{4-}$) and hydroxylated (Fe^{3+}-OH^-CDTA^{4-}) species will be investigated in relation with the pH and the ionic strength, which were adjusted through addition of sodium chloride, sodium sulfate, and lithium chloride electrolytes. Temperature was maintained at (25 ± 1) °C.

$$Fe^{3+}CDTA^{4-} + OH^- \leftrightarrow Fe^{3+}OH^-CDTA^{4-} \quad (4)$$

* To whom inquiries should be directed. Telephone: 1-418-656-3566. Fax: 1-418-656-5993. E-mail: faical.larachi@gch.ulaval.ca.

10.1021/je0341007 CCC: $25.00
Published on Web 10/14/2003

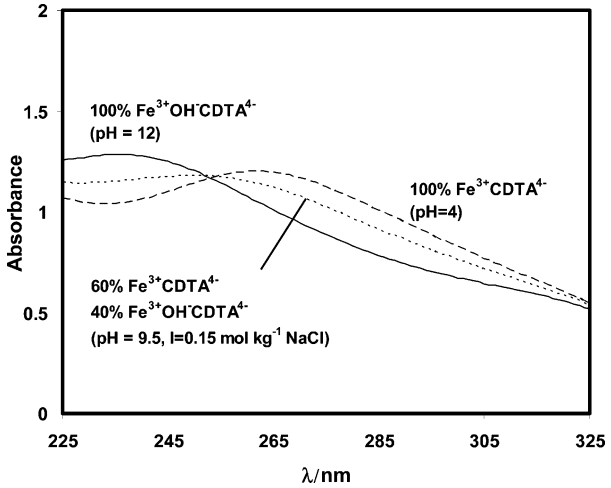

Figure 1. UV light spectra (225 to 325 nm) for individual $Fe^{3+}CDTA^{4-}$ and $Fe^{3+}OH^{-}CDTA^{4-}$ species with an example of combinatory spectra ($[Fe^{3+}] = 0.15$ mM).

The thermodynamic equilibrium constant (K, $pK = \log(K)$) is calculated via the measured stoichiometric equilibrium constant (K_C, $pK_C = \log(K_C)$) and knowledge of the species activity coefficients (γ_i):

$$K = \left(\frac{\gamma_{S2}}{\gamma_{S1}\gamma_{OH^-}}\right)\left(\frac{C_{S2}}{C_{S1}C_{OH^-}}\right) = K_\gamma K_C \qquad (5)$$

in which S1 and S2 stand for $Fe^{3+}CDTA^{4-}$ and $Fe^{3+}OH^{-}CDTA^{4-}$, respectively. Several models have been developed to represent as accurately as possible the activity coefficients quotient (K_γ, $pK_\gamma = -\log(K_\gamma)$). In this work, the well-known Hückel,[8,9] Bromley,[8,10,11] Scatchard,[9,12,13] and Pitzer[8,14,15] activity coefficient models will be compared to the experimental measurements.

Experimental Section

Ferric CDTA stock solutions were prepared using the following recipe: (1) (4.55 ± 0.05) g of *trans*-1,2-diaminocyclohexane-*N*,*N*,*N*′,*N*′ tetraacetic acid monohydrate powder (ACS grade−Aldrich Chemical) was dissolved into (325 ± 3) mL of 0.1 M NaOH solution; (2) after total CDTA dissolution, (2.50 ± 0.03) g of ferrous chloride tetrahydrate (Sigma) was added to the solution, resulting in an equimolar amount of dissolved Fe^{2+} and CDTA; (3) the stock solution was thoroughly mixed and left in the open air for 1 day, allowing Fe^{2+} conversion into Fe^{3+}. The final concentration of the $Fe^{3+}CDTA^{4-}$ stock solution was (38.5 ± 0.6) mM with a pH approaching 4.

Quantitative measurement of ferric CDTA was carried out with a UV−vis spectrophotometer (Varian Cary 300 model). $Fe^{3+}CDTA^{4-}$ and $Fe^{3+}OH^{-}CDTA^{4-}$ species generate different UV absorbance spectra in the (225 to 325) nm band (Figure 1). Prior to the study, calibration measurements were done in order to determine the spectra-to-concentration relationship for individual species. At ionic strengths approaching zero, two sets of fifteen (225 to 325) nm spectra for different $Fe^{3+}CDTA^{4-}$ (or $Fe^{3+}OH^{-}CDTA^{4-}$) concentrations of (0.01 to 0.40) mM were obtained and processed using *PLSplus IQ* principle component regression (PCR) analysis from *Thermo Galactic Grams/32 AI* software. Calibration measurements were done at pH boundaries where 100% of the non-hydroxylated species (pH = 4) and 100% of the hydroxylated species (pH = 12) could be observed.

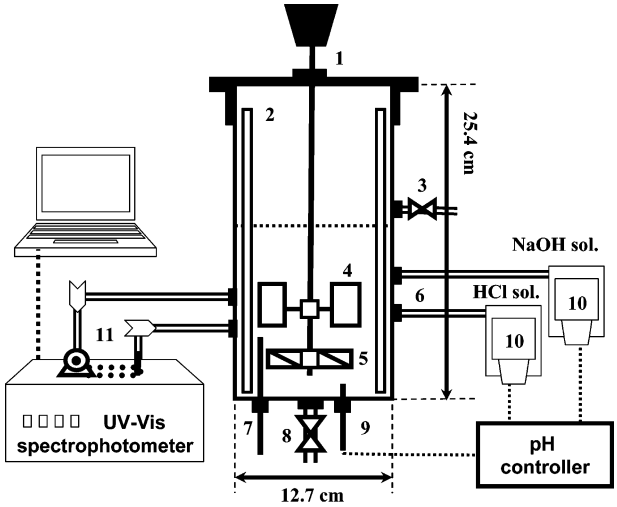

Figure 2. Stirred cell reactor with appendices: 1, rotor; 2, baffles; 3, solution inlet valve; 4, radial liquid stirrer; 5, axial liquid stirrer; 6, makeup acid and base inlet; 7, thermistor; 8, solution outlet valve; 9, pH probe; 10, volumetric pumps; 11, peristaltic pump (Varian Routine Sampler Accessory).

The equilibrium experiments were conducted in a Plexiglas stirred cell of 12.7 cm i.d. and 25.4 cm high (Figure 2). Radial and axial six-bladed turbine stirrers (6.35 cm i.d.) were centrally located in the aqueous media at a distance of 2.5 cm (axial stirrer) and 5 cm (radial stirrer) from the bottom. Four symmetrically mounted baffles increased the stirring efficiency and prevented vortex formation. For each trial, (6 ± 0.06) mL of the ferric CDTA stock solution was added to (1500 ± 15) mL of NaCl, Na_2SO_4, or LiCl electrolytic solution of specified ionic strength of ($1.5 \times 10^{-4} < I < 2.0$) mol kg^{-1}. This led to a diluted ferric CDTA concentration of (0.150 ± 0.002) mM which was inserted in the stirred cell. Notice that NaCl, Na_2SO_4, and LiCl salts were selected in this investigation because Na^+, Li^+, SO_4^{2-}, and Cl^- ions do not absorb UV light in the (225 to 325) nm band, thus avoiding awkward spectra interference. For each trial, a sequence of nine spectra was captured at pH ranging from 6 to 11. This was achieved via a pH controller (Liquitron DP5000, LMI Milton Roy) connected to a probe inserted in the cell. NaOH and HCl solutions of (0.1 ± 0.002) M were employed for pH control. After the required pH was attained, a sample of the investigated solution was extracted from the stirred cell via a peristaltic pump (Varian Routine Sampler Accessory) and rerouted to the spectrophotometer in-line cavity for reading. Replications were done to ensure spectral quality.

Experimental Results

Spectral analysis was performed with a previously established PCR calibration model on ferric CDTA. The respective $Fe^{3+}CDTA^{4-}$ and $Fe^{3+}OH^{-}CDTA^{4-}$ concentrations over the entire pH range were plotted on an equilibrium diagram. Such a typical distribution between $Fe^{3+}CDTA^{4-}$ and $Fe^{3+}OH^{-}CDTA^{4-}$ concentrations is illustrated in Figure 3 for an ionic strength of (0.50 ± 0.01) mol kg^{-1}. With knowledge of ferric CDTA species and hydroxide concentrations, the stoichiometric equilibrium constant was calculated according to eq 5. Table 1 gives a summary of the averaged pK_C values for each studied solution. As depicted in Figure 3, only pK_C values for which $Fe^{3+}CDTA^{4-}$ and $Fe^{3+}OH^{-}CDTA^{4-}$ concentrations exceeded 10% of the total ferric concentration were taken into account. Other measurements were discarded from further analysis, considering that slight but consistent spectral inaccuracies

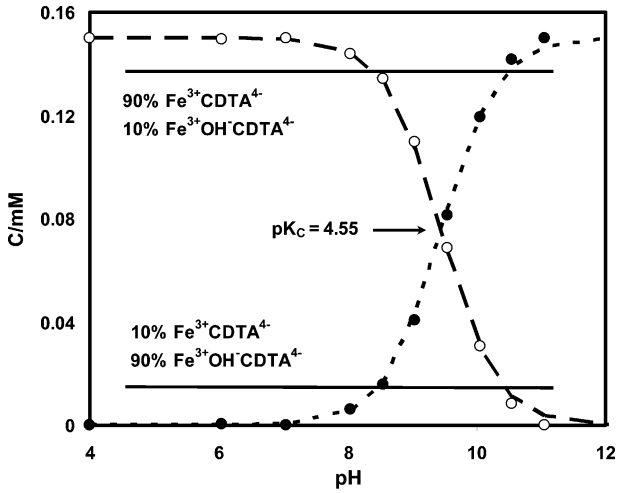

Figure 3. Concentration of non-hydroxylated and hydroxylated ferric CDTA species as a function of pH ($T = 298$ K, NaCl solution of $I = 0.5$ mol kg^{-1}).

Table 1. Averaged Stoichiometric Equilibrium Constant (pK_C) (± Standard Deviation on 3−5 Values) for the Fe^{3+}CDTA/$Fe^{3+}OH^-$CDTA Pair in NaCl, Na_2SO_4, and LiCl Solutions of Various Ionic Strength

	stoichiometric equil const (pK_C)		
I/mol kg^{-1}	NaCl	Na_2SO_4	LiCl
$(1.54-5.08) \times 10^{-4}$ [a]	4.351 ± 0.034		
$(5.35-8.88) \times 10^{-4}$ [a]	4.252 ± 0.055		
$(2.25-2.60) \times 10^{-3}$ [a]	4.203 ± 0.047		
$(5.31-5.49) \times 10^{-3}$ [a]	4.162 ± 0.039		
$1.03 \times 10^{-2} \pm 2 \times 10^{-4}$	4.126 ± 0.019	4.218 ± 0.017	4.230 ± 0.060
$2.55 \times 10^{-2} \pm 5 \times 10^{-4}$	4.161 ± 0.044		
$5.02 \times 10^{-2} \pm 1 \times 10^{-3}$	4.179 ± 0.047	4.236 ± 0.017	4.208 ± 0.024
$7.53 \times 10^{-2} \pm 1.5 \times 10^{-3}$	4.211 ± 0.025		
0.1 ± 0.002	4.258 ± 0.025	4.256 ± 0.024	4.312 ± 0.037
0.125 ± 0.0025	4.285 ± 0.025		
0.15 ± 0.003	4.328 ± 0.027		
0.2 ± 0.004	4.398 ± 0.008		
0.25 ± 0.005		4.364 ± 0.016	4.494 ± 0.039
0.3 ± 0.006	4.462 ± 0.018		
0.35 ± 0.007	4.501 ± 0.022		
0.5 ± 0.01	4.558 ± 0.040	4.445 ± 0.021	4.679 ± 0.042
0.75 ± 0.015	4.642 ± 0.042	4.499 ± 0.022	4.763 ± 0.037
1.0 ± 0.02	4.726 ± 0.029	4.534 ± 0.021	4.894 ± 0.038
1.5 ± 0.03	4.850 ± 0.018	4.575 ± 0.044	5.013 ± 0.040
2.0 ± 0.04	4.914 ± 0.026	4.722 ± 0.037	5.100 ± 0.070

[a] The presence of an ionic strength range is due to the addition of NaOH solution while adjusting the required pH.

could lead to high K_C discrepancies, especially in those regions where $Fe^{3+}CDTA^{4-}$ or $Fe^{3+}OH^-CDTA^{4-}$ concentrations approach zero.

Activity Coefficients Modeling

As illustrated from eq 5, the thermodynamic equilibrium constant related to the stoichiometric equilibrium constant is corrected by an activity coefficient quotient (K_γ). Models evaluating such quotients have been developed over the years, among which the Debye−Hückel limiting law has been the cornerstone of recent modeling attempts.

Hückel Equation. The extended Debye−Hückel equation is only applicable at very low ionic strengths (Figure 4). As a result, Hückel added a *salting-out* term accounting for the lowered salt solubilities at high ionic strength[8]

$$\mathrm{p}K_\gamma = \frac{A_\phi \Delta z^2 \sqrt{I}}{1+\sqrt{I}} - \epsilon I \qquad (6)$$

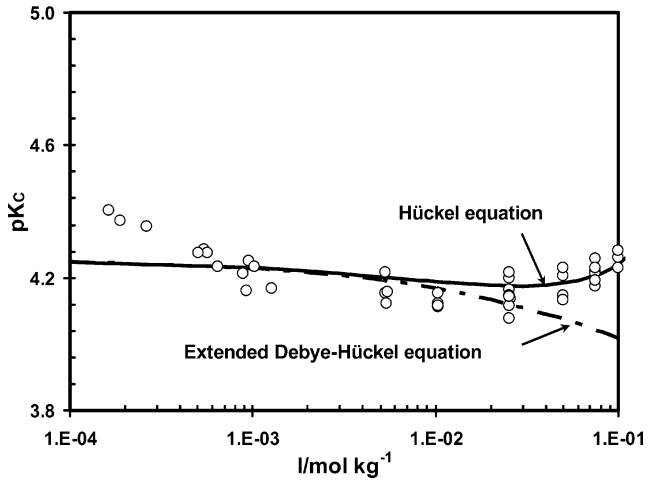

Figure 4. pK_C values vs the ionic strength for NaCl solutions of $I < 0.1$ mol kg^{-1}.

Table 2. Best Fitted pK and Activity Coefficient Model Parameters (AAE Is the Average Absolute Error on the Stoichiometric Equilibrium Constant)

	NaCl	Na_2SO_4	LiCl
Hückel equation			
pK	4.259	4.334	4.298
salting-out const, ϵ/(kg mol^{-1})	2.247	1.527	2.176
AAE ($0 < I < 2$ mol kg^{-1})	0.393	0.603	0.798
AAE ($0 < I < 0.25$ mol kg^{-1})	0.039	0.020	0.030
Bromley models			
pK	4.256	4.297	4.263
ion−ion interaction const, B_1/(mol kg^{-1})	6.933	2.872	9.469
ion−ion interaction const, B_2	13.648	11.344	19.047
arbitrary const, α/(kg$^{0.5}$ mol$^{-0.5}$)	1.000	0.574	1.000
AAE ($0 < I < 2$ mol kg^{-1})	0.057	0.023	0.122
AAE ($0 < I < 1$ mol kg^{-1})	0.033	0.016	0.036
Scatchard expansion			
pK	4.275	4.302	4.280
linear term coefficient, C_1/(kg mol^{-1})	−2.103	−1.861	−2.410
quadratic term coefficient, C_2/(kg^2 mol^{-2})	1.884	1.890	2.101
ternary term coefficient, C_3/(kg^3 mol^{-3})	−0.622	−0.649	−0.679
AAE ($0 < I < 2$ mol kg^{-1})	0.053	0.077	0.090
AAE ($0 < I < 1.5$ mol kg^{-1})	0.036	0.024	0.033
Pitzer model			
pK	4.284	4.302	4.291
ion interaction summation, $\sum\beta^0_\pm$	−0.367	−0.367	0.121
ion interaction summation, $\sum\beta^1_\pm$	−5.522	−5.522	−5.95
ion interaction coefficient, β^1_{salt}	−3.690	−4.978	−0.226
AAE ($0 < I < 2$ mol kg^{-1})	0.038	0.027	0.037

where A_ϕ, the Debye−Hückel parameter, equals 0.509 at the temperature 25 °C[16] and $\Delta z^2 = 4$ for the present species (see eq 4). *Salting-out* constants, ϵ/(kg mol^{-1}), for each electrolyte are given in Table 2. This equation is relatively successful for solutions up to 0.1 M ionic strength.[8] Yet, a good fit of the Hückel equation over the present measurements can be extended to 0.25 M (see Figures 4 and 5).

Bromley Models. Bromley improved the Hückel equation by adding specific ion−ion interaction terms which become more significant at high electrolyte concentration.[10,11] For uni-univalent salts (i.e. NaCl, LiCl), Bromley proposed the following relationship:

$$\mathrm{p}K_\gamma = \frac{A_\phi \Delta z^2 \sqrt{I}}{1+\sqrt{I}} - B_1 I - \frac{(0.06+0.6B_1)\Delta z^2}{(1+3I/2\Delta z^2)^2} I + B_2 \alpha \sqrt{I}\{1-\exp(-\alpha\sqrt{I})\} \qquad (7)$$

where B_1/(mol kg^{-1}) and B_2 are empirical ion−ion interac-

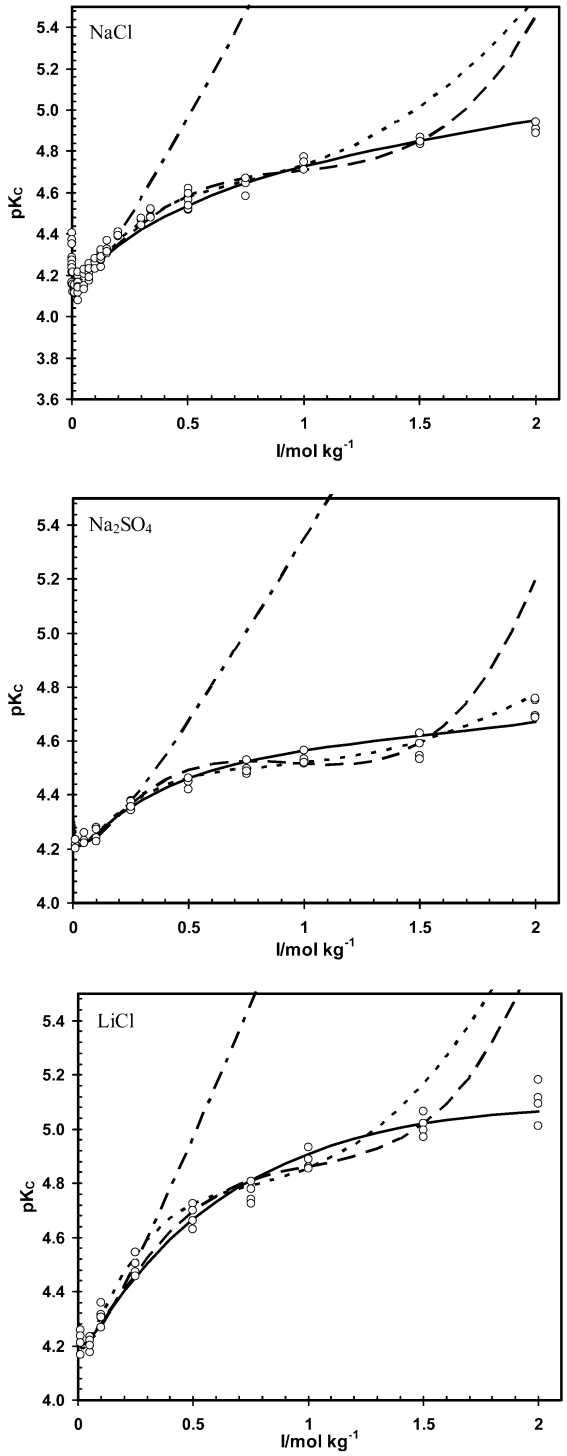

Figure 5. pK_C values vs the ionic strength for NaCl, Na_2SO_4, and LiCl solutions according to several activity coefficient models: - – -, Hückel; - - -, Bromley; – – –, Scatchard; —, Pitzer.

tion constants and $\alpha/(kg^{0.5}\ mol^{-0.5})$ is an arbitrary constant which is set to 1 for uni-univalent electrolytes. For uni-divalent salts (i.e. Na_2SO_4), Bromley recommended another form instead of eq 7.

$$pK_\gamma = \frac{A_\phi \Delta z^2 \sqrt{I}}{1+\sqrt{I}} - B_1 I - \frac{(0.06 + 0.6B_1)\Delta z^2}{(1 + 3I/2\Delta z^2)^2} I + B_2 \ln(1 + \alpha^2 I) \quad (8)$$

Here the arbitrary constant α must be fitted simultaneously with the ion−ion interaction parameters. For the case involving Na_2SO_4, α was determined to approach 0.574 (see Table 2). The model's general aptitude to predict pK_C via knowledge of pK_γ and a pK is tolerable in the 0−2 M ionic strength extent (average absolute error of 0.023 < AAE < 0.122; Table 2). However, it is clear that, for NaCl and LiCl solutions, Bromley's model cannot be effectively applied for I values greater than 1 (Figure 5). Indeed, the model's applicability seems to differ from one electrolyte to the other.

Scatchard Expansion. The Scatchard model[9,13] establishes itself on a variation of the Debye−Hückel limiting law upon which a power series expansion in I is appended.

$$pK_\gamma = \frac{2S}{\ln(10)}\left(\frac{\sqrt{I}}{1+1.5\sqrt{I}}\right) + C_1 I + C_2 I^2 + C_3 I^3 \quad (9)$$

where $S = 1.172$ for solutions at 25 °C[13] and $C_1/(kg\ mol^{-1})$, $C_2/(kg^2\ mol^{-2})$, and $C_3/(kg^3\ mol^{-3})$ are fitted power series coefficients given in Table 2. As shown in Figure 5, it seems that the actual ternary expansion on the ionic strength is adequate for electrolytic solutions of low-to-moderate concentration (I < 1.5 M) with a fitting discrepancy (0.024 < AAE < 0.036 ; Table 2) remaining well within the accepted limits (AAE < 0.05).[17] Still, the model's applicability over a broader range of ionic strength would require further modification of its current structure.

Pitzer Model. Pitzer's more comprehensive formulation of the activity coefficient uses a *modified* Debye−Hückel limiting law coupled with complex exponential functions which take into account individual cation/anion binary interactions ($\beta^0_\pm$, $\beta^1_\pm$).[8,14−15]

$$pK_\gamma = \frac{A_\phi \Delta z^2}{\ln(10)}\left(\frac{\sqrt{I}}{1+1.2\sqrt{I}} + \frac{5}{3}\ln(1+1.2\sqrt{I})\right) + \frac{2I}{\ln(10)}\{\sum\beta^0_\pm + \beta^1_{salt}\exp(-2\sqrt{I})\} + \frac{\sum\beta^1_\pm - \beta^1_{salt}}{\ln(10)}\{1-(1+2\sqrt{I})\exp(-2\sqrt{I})\} \quad (10)$$

with

$$\sum\beta^0_\pm = \beta^0_{X,S2} + \beta^0_{X,S1} + \beta^0_{X,OH}$$

and

$$\sum\beta^1_\pm = \beta^1_{X,S2} + \beta^1_{X,S1} + \beta^1_{X,OH}$$

where X stands for Na^+ or Li^+ while β^1_{salt} corresponds to the Pitzer interaction coefficient for ions emanating from the electrolyte (i.e. $\beta^1_{salt} \equiv \beta^1_{Na^+,Cl^-}$ for NaCl). Application of the Pitzer model over experimental measurements was achieved upon fitting of the cation−anion interaction coefficient summations ($\Sigma\beta^0_\pm$, $\Sigma\beta^1_\pm$) and the specific electrolyte coefficient β^1_{salt} (see Table 2). Considering that anion−anion and cation−cation interactions are neglected and that all species involved in the equilibrium are negatively charged (eq 4), it must be understood that the corresponding $\Sigma\beta^0_\pm$ and $\Sigma\beta^1_\pm$ summations for NaCl and Na_2SO_4 trials are equivalent, since they involve interactions with Na^+, common in both electrolytes. In this case, the remaining fitting parameter β^1_{salt} is widely sufficient to discriminate K_γ predictions for NaCl and Na_2SO_4 solutions. Finally, Pitzer showcases the most appropriate fit

of all K_γ models over the entire experimental conditions (I < 2 mol kg^{-1}) with an AAE < 0.038 for all electrolytes.

Conclusions

This work was intended to measure the acid−base thermodynamic equilibrium constant (K) for the Fe^{3+}-$CDTA^{4-}$/$Fe^{3+}OH^-CDTA^{4-}$ pair by means of the measured concentrations and calculation of the activity coefficient quotient in electrolyte solutions of NaCl, Na_2SO_4, and LiCl at (298 ± 1) K. In conjunction with Hückel, Bromley, Scatchard, and Pitzer's K_γ predictions, the averaged K value over 150 K_C measurements is 1.94×10^4 with a standard deviation of 1.0×10^3 (pK = 4.288 ± 0.022). Good fit of the K_C measurements was achieved in the following ionic strength regions: Hückel (I < 0.25 mol kg^{-1}), Bromley (I < 1 mol kg^{-1}), Scatchard (I < 1.5 mol kg^{-1}), Pitzer (I < 2 mol kg^{-1}). In those instances, the predictions presented acceptable fitting discrepancies well within the accepted limits (average absolute error on pK_C < 0.05).

Literature Cited

(1) Wubs, H. J.; Beenackers, A. C. M. Kinetics of H_2S absorption into aqueous ferric solutions of EDTA and HEDTA. *AIChE J.* **1994**, *40*, 433−444.

(2) Demminck, J. F.; Beenackers, A. C. M. Gas desulfurisation with ferric chelates of EDTA and HEDTA: New model for the oxidative absorption of hydrogen sulfide. *Ind. Eng. Chem. Res.* **1998**, *37*, 1444−1453.

(3) Martell, A. E.; Motekaitis, R. J.; Chen, D.; Hancock, R. D.; McManus, D. Selection of new Fe(III)/Fe(II) chelating agents as catalysts for the oxidation of hydrogen sulfide to sulfur by air. *Can. J. Chem.* **1996**, *74*, 1872−1879.

(4) Philip, C. V.; Brooks, D. W. Iron(III) chelate complexes of hydrogen sulfide and mercaptans in aqueous solution. *Inorg. Chem.* **1974**, *13*, 384−386.

(5) Phillips, D. J.; Phillips, S. L. High-temperature dissociation constants of HS^- and the standard thermodynamic values for S^{2-}. *J. Chem. Eng. Data* **2000**, *45*, 981−987.

(6) Gustafson, R. L.; Martell, A. E. Hydrolytic tendencies of ferric chelates. *J. Phys. Chem.* **1963**, *67*, 576−582.

(7) Wilkins, R. G.; Yelin, R. E. The kinetics of monomer−dimer interconversion of iron(III) ethylene diaminetetraacetate and related chelates. *Inorg. Chem.* **1969**, *8*, 1470−1473.

(8) Zemaitis, J. F., Jr.; Clark, D. M.; Rafal, M.; Scrivner, N. C. *Handbook of aqueous electrolyte thermodynamics*; AIChE: New York, 1986.

(9) Alonso, P.; Barriada, P.; Rodriguez, I.; Sastre de Vicente, M. E. Acid−base equilibrium constants for glycine in $NaClO_4$, KCl, and KBr at 298 K. Dependence on ionic strength. *J. Chem. Eng. Data* **1998**, *43*, 876−879.

(10) Bromley, L. A. Approximate individual ion values of β in extended Debye−Hückel theory for uni-univalent aqueous solutions at 298.15 K. *J. Chem. Thermodyn.* **1972**, *4*, 669−675.

(11) Bromley, L. A. Thermodynamic properties of strong electrolytes in aqueous solutions. *AIChE J.* **1973**, *19*, 313−317.

(12) Scatchard, G. Osmotic coefficients and activity coefficients in mixed electrolyte solutions. *J. Am. Chem. Soc.* **1961**, *83*, 2636−2642.

(13) Brandaritz, I.; Fiol, S.; Herrero, R.; Vilarino, T.; Sastre de Vicente, M. Protonation constants of α-alanine, γ-aminobutyric acid, and ϵ-aminocaproic acid. *J. Chem. Eng. Data* **1993**, *38*, 531−533.

(14) Pitzer, K. S. Thermodynamics of electrolytes. I. Theoretical basis and general equations. *J. Phys. Chem.* **1973**, *77*, 268−276.

(15) Pitzer, K. S. *Activity Coefficients in Electrolyte Solutions*; CRC Press Inc.: Boca Raton, FL, 1991; Chapter 3.

(16) Bradley, D. J.; Pitzer, K. S. Thermodynamics of electrolytes. 12. Dielectric properties of water and Debye−Hückel parameters to 350 °C and 1 kbar. *J. Phys. Chem.* **1979**, *83*, 1599−1603.

(17) Albert, A.; Serjeant, E. P. *The Determination of Ionization Constant, A Laboratory Manual*, 3rd ed.; Chapman and Hall: London, New York, 1984.

Received for review May 30, 2003. Accepted September 8, 2003. Financial support from the Natural Sciences and Engineering Research Council of Canada (NSERC) and the Fonds Québécois de la Recherche sur la Nature et les Technologies is gratefully acknowledged.

JE0341007